Maturation of layer 5 neocortical pyramidal neurons: amplifying salient layer 1 and layer 4 inputs by Ca^{2+} action potentials in adult rat tuft dendrites

J. Julius Zhu

Abteilung Zellphysiologie, Max-Planck-Institut für medizinische Forschung, Jahnstrasse 29, D-69120 Heidelberg, Germany

(Received 7 March 2000; accepted after revision 3 May 2000)

1. Changes in the arborization and electrical excitability of the apical dendritic tufts of pyramidal cells of cortical layer 5 were examined during the first 2 months (postnatal days (P)2–56) of postnatal development in rats.

2. Reconstructions of biocytin-filled neurons showed that the apical dendritic trunk was continually growing, becoming longer and thicker and that the distance between the tuft and soma increased more than 5-fold.

3. In P2 animals, both the tuft and soma had a high input resistance (>500 MΩ) and the tuft was electrotonically close to the soma. In contrast, the apical tuft and soma of P56 neurons had a low input resistance (<50 MΩ) and they were electrotonically isolated from each other.

4. Depolarizing current pulses injected into the tuft of P2 cells generated mostly Na^+-dependent regenerative dendritic potentials of short duration (~15 ms) while in the tuft of P56 animals, complex regenerative potentials were generated which had a longer duration (~55 ms) and were Na^+ and Ca^{2+} dependent. In young and juvenile animals (P14–28) dendritic regenerative potentials could be restricted to the apical dendritic tuft whereas in adult animals ($>$P42), the complex regenerative potentials frequently occurred simultaneously with somatic action potentials.

5. The main developmental change in layer 5 pyramidal neurons, as assayed with square pulse current injections and synaptic stimulations, is the progressive electrotonic isolation of the dendritic tuft from the soma. This change is concomitant with the appearance of complex, mostly Na^+- and Ca^{2+}-dependent, regenerative dendritic potentials initiated partly in the tuft and partly in the axon. The coupling of the dendritic tuft and axonal initiation zones for regenerative potentials by active dendritic Na^+ and Ca^{2+} conductances enables mature layer 5 pyramidal neurons to detect selectively the salient distal synaptic inputs and coincident synaptic inputs arriving at different cortical layers.

Layer 1, the most superficial layer of the neocortex, is primarily a synaptic zone containing mostly asymmetric, presumably excitatory synapses (Jones & Powell, 1970; Vaughan & Peters, 1973). Most inputs to layer 1 originate from the higher-order cortical areas (Zeki & Shipp, 1988; Johnson & Burkhalter, 1997; Cauller *et al.* 1998), cholinergic and monoaminergic systems (De Lima & Singer, 1986; Lysakowski *et al.* 1986), and secondary sensory ascending system (Herkenham, 1980; Jones, 1998). Activity of the layer 1 inputs may be associated with attention, perception and learning (Cauller & Kulics, 1988; Squire & Zola-Morgan, 1991). Most layer 1 fibres form synapses on the dendritic spines of layer 2/3 and layer 5 pyramidal cells (Jones & Powell, 1970; Vaughan & Peters, 1973). When activated, these synapses can generate large EPSPs that evoke action potentials in the axon of pyramidal cells (Cauller & Connors, 1994).

The large pyramidal cells of layer 5 can have a layer 1-projecting apical dendrite that extends over 1 mm. How the very distal synaptic inputs are transmitted to the axonal integration site of a layer 5 neuron is not fully understood. Previous studies have shown that the apical dendrite of pyramidal neurons in the hippocampus and neocortex has regenerative conductances (e.g. Chang, 1952; Spencer & Kandel, 1961; Wong *et al.* 1979; Regehr *et al.* 1993; Amitai *et al.* 1993). It has been suggested that these dendritic conductances amplify the distal synaptic inputs in the apical dendrites (Kim & Connors, 1993; Cauller & Connors 1994; Magee & Johnston, 1995; Schwindt & Crill, 1995; Gillessen & Alzheimer, 1997; Zhu & Connors, 1999). Recent evidence from juvenile (P28) animals indicates that layer 5 neocortical pyramidal neurons have a functionally separate dendritic zone enriched with active conductances for integrating and amplifying distal synaptic inputs (Schiller *et al.* 1997).

Neocortical neurons undergo an extensive change in their dendritic morphology during postnatal development (e.g. Petit *et al.* 1988; Kasper *et al.* 1994). Anatomical measurements suggest that the development of dendritic morphology, such as the apical dendrite of layer 5 pyramidal cells in the rat, can be roughly divided into three stages, each lasting about 2 weeks (Petit *et al.* 1988). During the 1st and 2nd postnatal weeks, the apical dendrite has the highest growth rate, becoming nearly mature in a relatively short period. During the 3rd and 4th postnatal weeks, the apical dendrite elongates further to reach its mature length of over 1 mm. During the subsequent 2 weeks, the width of the apical dendrite increases continually into adulthood. Since the membrane properties may play an important role in signalling between the subcellular compartments of layer 5 pyramidal neurons, we examined changes in the electrical properties of the dendritic tuft concomitantly with anatomical maturation. We found that both the morphological and physiological properties of layer 5 pyramidal cells in the rat neocortex matured in the first 6 postnatal weeks. This study has previously been presented in abstract form (Zhu & Sakmann, 1997).

METHODS

Slice preparation

Experiments were performed in somatosensory neocortical slices from P2–56 Wistar rats. The brain slices were prepared as previously described (Zhu & Lo, 1999). All animal procedures were carried out according to the animal welfare guidelines of the Max Planck Society. In brief, the rats were deeply anaesthetized with halothane and decapitated. Tissue blocks containing the somatosensory cortex were quickly removed into cold (0–4 °C), oxygenated physiological solution containing (mM): NaCl 125, KCl 2·5, NaH_2PO_4 1·25, $NaHCO_3$ 25, $MgCl_2$ 1, dextrose 25, $CaCl_2$ 2, at pH 7·4. The removal procedure was performed as quickly as possible (within 10 s), this appeared to be crucial for obtaining healthy slice tissues from the adult animals (> P42). Sagittal slices, 250–300 μm thick, were then cut from the tissue blocks in cold (0–4 °C), oxygenated physiological solution, using a microslicer (Campden Instruments Ltd, UK) set at the slowest possible advancing speed. The slices were then kept in warm (37·0 ± 0·5 °C), oxygenated physiological solution for about 1 h before recording. During recording, slices were submerged in a Plexiglass chamber and stabilized using a fine nylon net attached to a platinum ring, perfused with warmed and oxygenated physiological solution. The temperature of the bath solution in the chamber was kept at 35·0 ± 0·5 °C.

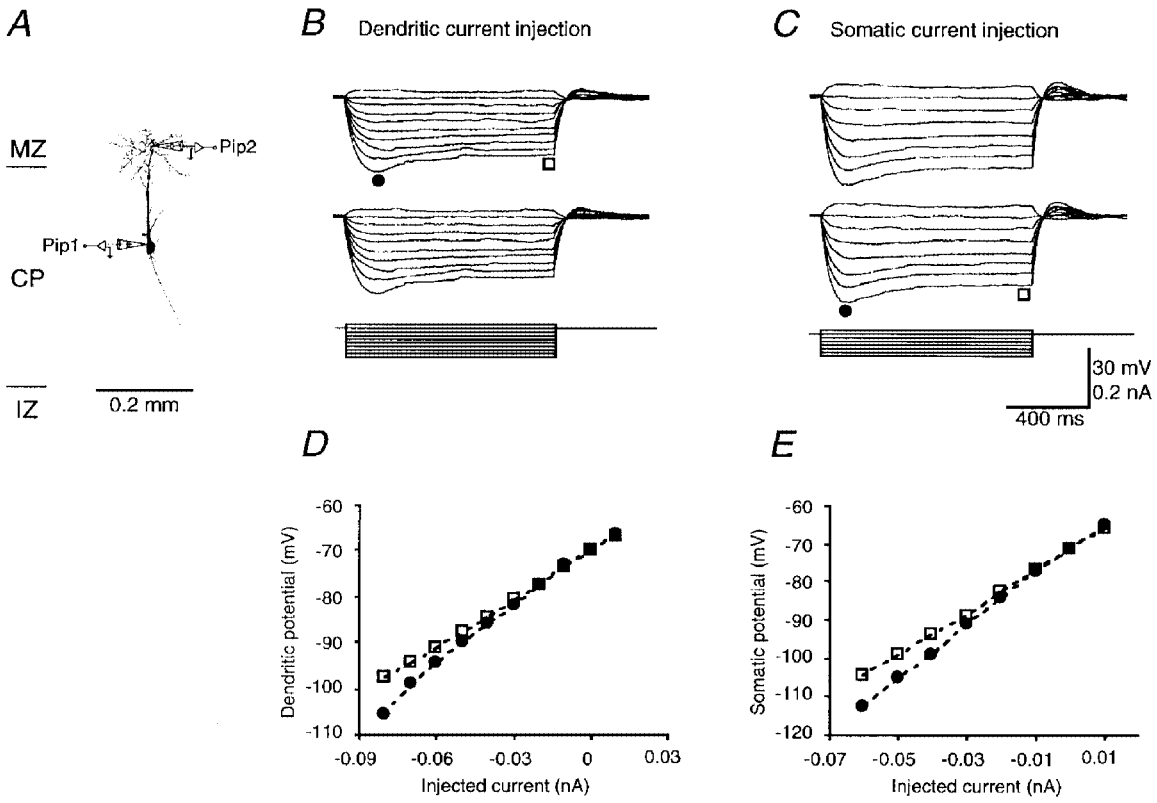

Figure 1. Membrane properties of a P2 pyramidal cell

A, morphology of a P2 pyramidal cell, reconstructed using Neurolucida. The schematic drawing of recording pipettes indicates the location of the dendritic (Pip 2, 203 μm distal from the soma) and somatic (Pip 1) recording. The length of the apical dendrite was 250 μm. MZ, marginal zone; CP, cortical plate; IZ, intermediate zone. *B* and *C*, dendritic (upper traces) and somatic (middle traces) responses to step current injections (lower traces) into the tuft and the soma, respectively. The scale bars apply to both *B* and *C*. *D* and *E*, early (● in *B* and *C*) and steady-state (□ in *B* and *C*) *I–V* relationships at the tuft and the soma, respectively. The resting membrane potential in the soma and dendrite was −71 and −70 mV, respectively. The input resistance at the soma and dendrite was 586 and 529 MΩ, respectively.

Physiology

Simultaneous somatic and dendritic recording was performed on single, identified layer 5 pyramidal neurons using infrared differential interference contrast optics. Individual tuft branches (0·5–4 μm in diameter), located as deep as ~75 μm from the slice surface, could be identified when the optical system was optimally adjusted. The dendritic recordings were made from a primary and/or a secondary tuft branch of the apical dendrite of the pyramidal neurons. Somatic (5–10 MΩ) and dendritic (10–25 MΩ) recording pipettes were filled with the standard intracellular solution containing (mM): potassium gluconate 115, Hepes 10, $MgCl_2$ 2, MgATP 2, Na_2ATP 2, GTP 0·3, KCl 20, and biocytin 0·25%, at pH 7·3. Whole-cell recordings were made with two Axoclamp-2B amplifiers (Axon Instruments). Dual recordings from the soma and tuft were typically stable throughout experiments and the recordings were terminated if cells showed sustained change in resting membrane potential or input resistance. The hyperpolarization-activated inward rectification was quantified by measuring the amplitude of the depolarizing sag induced by hyperpolarizing membrane potential to -100 ± 2 mV. The attenuation of voltage responses between the tuft and soma was measured by hyperpolarizing either the tuft or soma to -100 ± 2 mV with a long current pulse. The somatofugal and somatopetal voltage attenuations were typically very similar and the two were averaged. The membrane potential right before the initiation of a regenerative potential was taken as the voltage threshold. An 11 mV liquid junction potential was subtracted from all membrane potentials.

Synaptic stimulation was made using a concentric bipolar electrode with single voltage pulses (200 μs, up to 40 V, 0·25 Hz). The stimulating electrode was typically placed at the border of layer 1 and layer 2, 1200–1500 μm lateral from the cells. A surgical cut was made between the stimulating electrode and the cells, from the middle layer 2 to the white matter, 400–600 μm lateral from the cells (see Fig. 14*A*). This arrangement allowed us to activate the layer 1/2 synaptic inputs more selectively (cf. Cauller & Connors, 1994; see also Reyes & Sakmann (1999) for the possible activation of the layer 2/3 neuron-relayed inputs).

Histology

After recording, slices were fixed by immersion in 4% paraformaldehyde in 0·1 M phosphate buffer. The tissue sections were processed with the avidin–biotin–peroxidase method to reveal cell morphology. Cells were then drawn with the aid of a computerized reconstruction system (Neurolucida). The diameters of the apical dendrite were measured at the midpoint between the centre of the soma and the main branch point. Somatic membrane areas (SAs) were estimated from the formula $SA = \pi ab$, where a is the major diameter and b is the minor diameter of the soma. These values were obtained from the fixed slices after the cell morphology was recovered. Vertical distances of the dendritic recording from the soma and the lengths of the apical dendrite were measured during the recording and later from the fixed tissue. The values obtained from living slices were nearly identical to those measured from the fixed tissue, therefore, no shrinkage

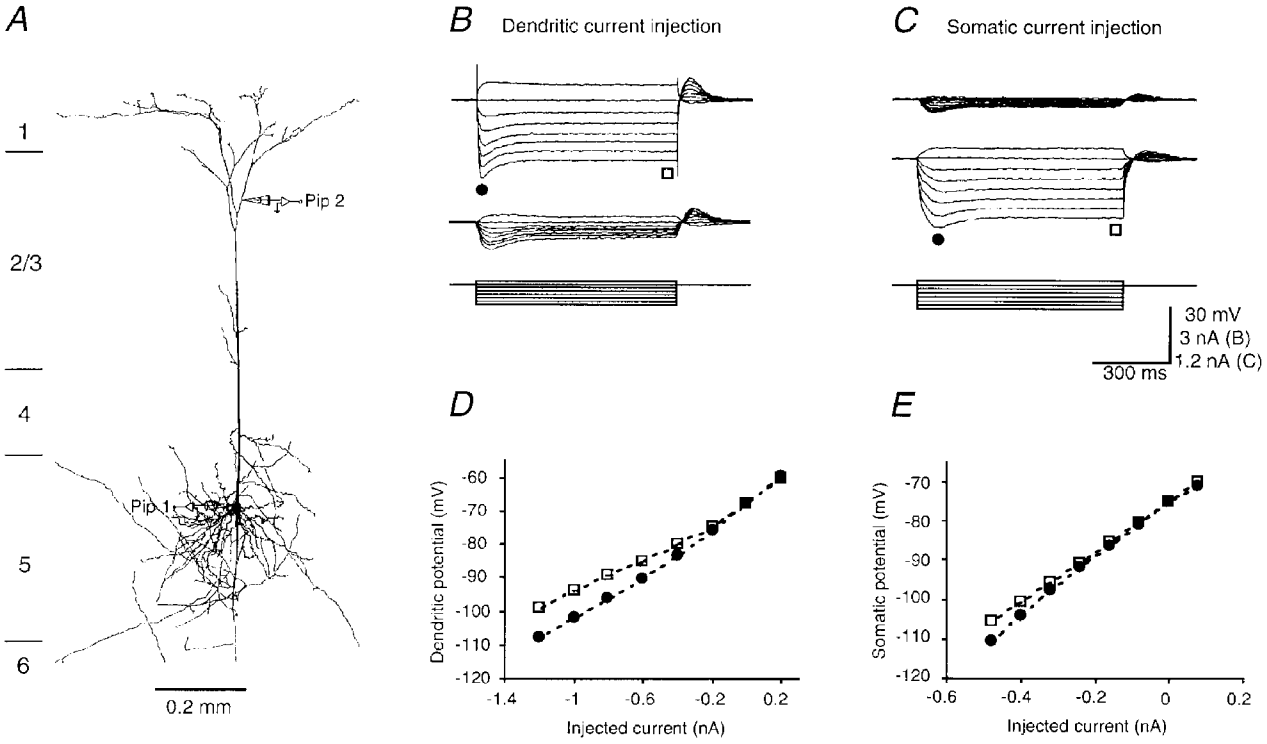

Figure 2. Membrane properties of a P14 pyramidal cell

A, morphology of a P14 pyramidal cell, reconstructed using Neurolucida. The schematic drawing of recording pipettes indicates the location of the dendritic (Pip 2, 667 μm distal from the soma) and somatic (Pip 1) recording. The length of the apical dendrite was 936 μm. *B* and *C*, dendritic (upper traces) and somatic (middle traces) responses to step current injections (lower traces) into the tuft and the soma, respectively. The scale bars apply to both *B* and *C*. *D* and *E*, early (● in *B* and *C*) and steady-state (□ in *B* and *C*) *I–V* relationships at the tuft and the soma, respectively. The resting membrane potential in the soma and dendrite was −73 and −69 mV, respectively. The input resistance at the soma and dendrite was 116 and 55 MΩ, respectively.

corrections were made for the diameters of the apical dendrite and SAs (cf. Stuart & Spruston, 1998).

RESULTS

Identification of pyramidal neurons at different postnatal ages

In slices of 2-day-old (P2) animals, whole-cell voltage recordings were made from pyramidal cells located in the cortical plate, where almost all cells at this developmental stage are destined to be layer 5 pyramidal cells (Berry & Rogers, 1965; Miller, 1981). In slices of 14- (P14), 28- (P28), 42- (P42) and 56-day-old (P56) animals the different cortical layers were readily distinguishable and recordings were made from identified, tufted layer 5 pyramidal cells.

Morphology and membrane properties of dendritic tuft

P2 cortex. Recordings were made from 10 pyramidal neurons in slices from P2 rats and the morphology of eight cells was recovered (Figs 1*A* and 7*A*). These cells had a small, ovoid soma, with a mean SA of $1307 \pm 398\ \mu m^2$ ($n = 8$; mean ± S.D.). They had an apical dendrite extending toward the pia mater, which bifurcated distally to form two elaborate dendritic tuft branches. The main apical dendrite was $219 \pm 130\ \mu m$ long ($n = 10$). The diameter of the apical dendrite, measured at the midpoint between the soma and primary branch point, was $2{\cdot}5 \pm 1{\cdot}0\ \mu m$ ($n = 8$). The P2 cells also had several basal dendrites and an axon, which had only a few, if any, secondary branches.

Dual dendritic and somatic recordings from P2 pyramidal cells showed that the tuft and soma had comparable resting membrane potentials and input resistances. The mean resting membrane potentials for the tuft and soma were $-71{\cdot}8 \pm 1{\cdot}4$ ($n = 10$) and $-72{\cdot}0 \pm 3{\cdot}9$ mV ($n = 10$), respectively. The input resistances, measured by injecting a small hyperpolarizing current, were 557 ± 202 ($n = 10$) and 625 ± 322 MΩ ($n = 10$), respectively. The resting membrane potentials and input resistances for the tuft and soma were not significantly different (Student's t test, $P > 0{\cdot}05$). In response to long (1 s) hyperpolarizing current injections, the membrane potential in both the tuft (Fig. 1*B*) and soma (Fig. 1*C*) of P2 cells exhibited small depolarizing 'sags', but the steady-state I–V relationships were almost linear (Fig. 1*D* and *E*). These depolarizing 'sags' suggest that P2 neurons possess hyperpolarization-activated cation and hyperpolarization-inactivated potassium conductances (e.g. I_h and I_M, respectively; McCormick & Prince, 1986;

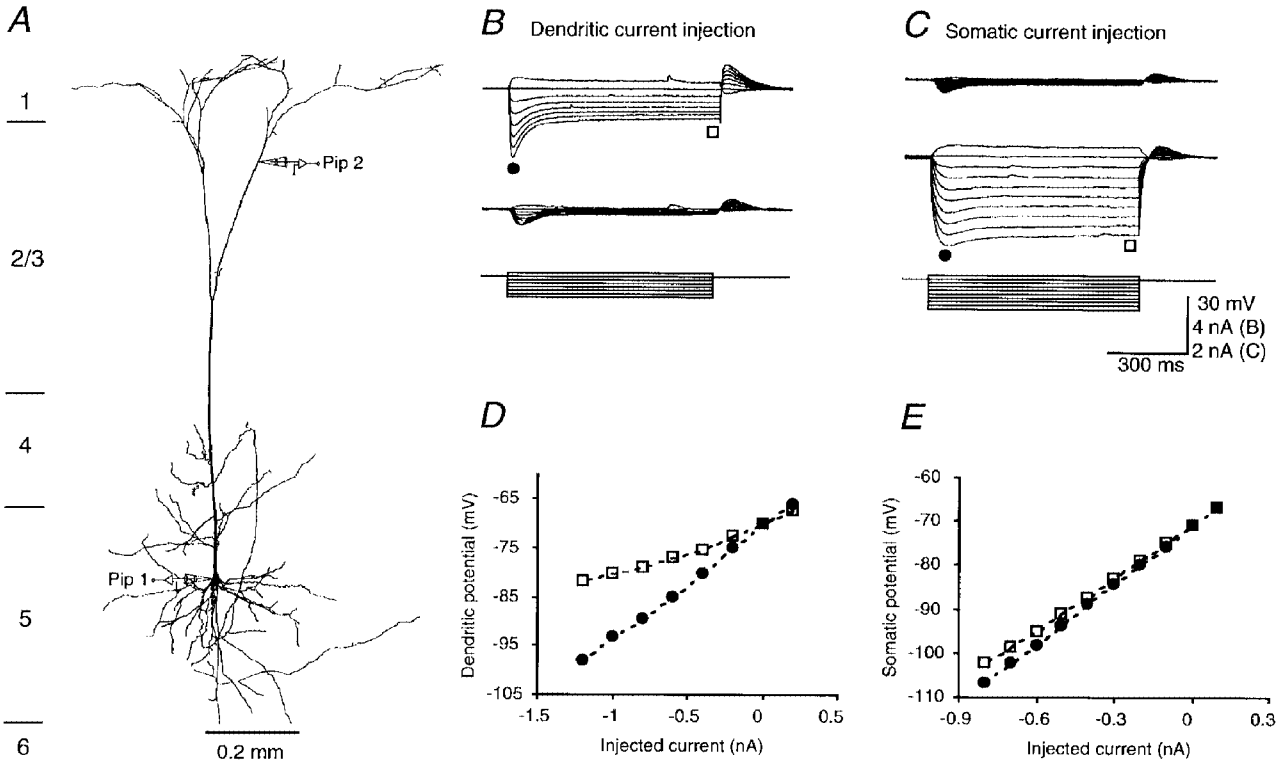

Figure 3. Membrane properties of a P28 pyramidal cell

A, morphology of a P28 pyramidal cell, reconstructed using Neurolucida. The schematic drawing of recording pipettes indicates the location of the dendritic (Pip 2, 904 μm distal from the soma) and somatic (Pip 1) recording. The length of the apical dendrite was 1185 μm. *B* and *C*, dendritic (upper traces) and somatic (middle traces) responses to step current injections (lower traces) into the tuft and the soma, respectively. The scale bars apply to *B* and *C*. *D* and *E*, early (● in *B* and *C*) and steady state (□ in *B* and *C*) I–V relationships at the tuft and the soma, respectively. The resting membrane potential in the soma and dendrite was −72 and −71 mV, respectively. The input resistance at the soma and dendrite was 41 and 20 MΩ, respectively.

Spain *et al.* 1987; Stuart & Spruston, 1998). The attenuation of responses measured either somatofugally or somatopetally (Fig. 1*B* and *C*, respectively) was small (2·0 ± 0·6 %; $n = 10$), indicating that P2 pyramidal cells were electrotonically very compact.

P14 cortex. We recorded from 14 pyramidal cells of P14 rats and recovered the morphology of 13 neurons (Figs 2*A* and 8*A*). Two weeks postnatally, layer 5 pyramidal cells had acquired many of their mature properties. The size of the soma had nearly doubled and the mean SA value was 2209 ± 496 μm^2 ($n = 13$). The apical dendrite was longer (1067 ± 94 μm; $n = 14$) and had a larger diameter (4·0 ± 0·9 μm; $n = 13$). The basal dendrites and axon were also longer and branched extensively (compare Figs 1*A* and 7*A* with Figs 2*A* and 8*A*).

The dendritic tuft and soma of P14 pyramidal cells had slightly different resting membrane potentials and input resistances. The resting membrane potential in the tuft was −68·5 ± 2·7 mV ($n = 16$), while that in the soma was −73·4 ± 2·4 mV ($n = 13$). The input resistance for the tuft was 50·6 ± 12·5 MΩ ($n = 16$), while that for the soma was 81·1 ± 12·7 MΩ ($n = 13$). The differences between these values were statistically significant ($P < 0·001$). In response to hyperpolarizing current injections, the tuft and soma of P14 cells showed clear depolarizing sags (Fig. 2*B* and *C*, respectively). Inward rectification was evident in the steady-state *I–V* relationships in the tuft (Fig. 2*B* and *D*), but not in the soma (Fig. 2*C* and *E*), suggesting a selective increase in hyperpolarization-activated cation conductances (e.g. I_h) in the tuft. In P14 neurons, the dendritic tuft was electrotonically more distant from the soma. This is reflected by the fact that the attenuation of the voltage response (53·4 ± 11·6 %; $n = 12$) between the soma and tuft was much greater in P14 than in P2 neurons in both directions (Figs 1 and 2).

P28 cortex. Pyramidal cells from 21 slices of P28 brains were examined and recovered (Figs 3*A* and 9*A*). These neurons had a pyramid-shaped soma with a mean SA of 2571 ± 489 μm^2 ($n = 21$), which was significantly larger than that of P14 cells ($P < 0·05$). The length and diameter of the apical dendrite had increased further to 1268 ± 87 ($n = 21$) and 4·8 ± 0·9 μm ($n = 21$), respectively, compared

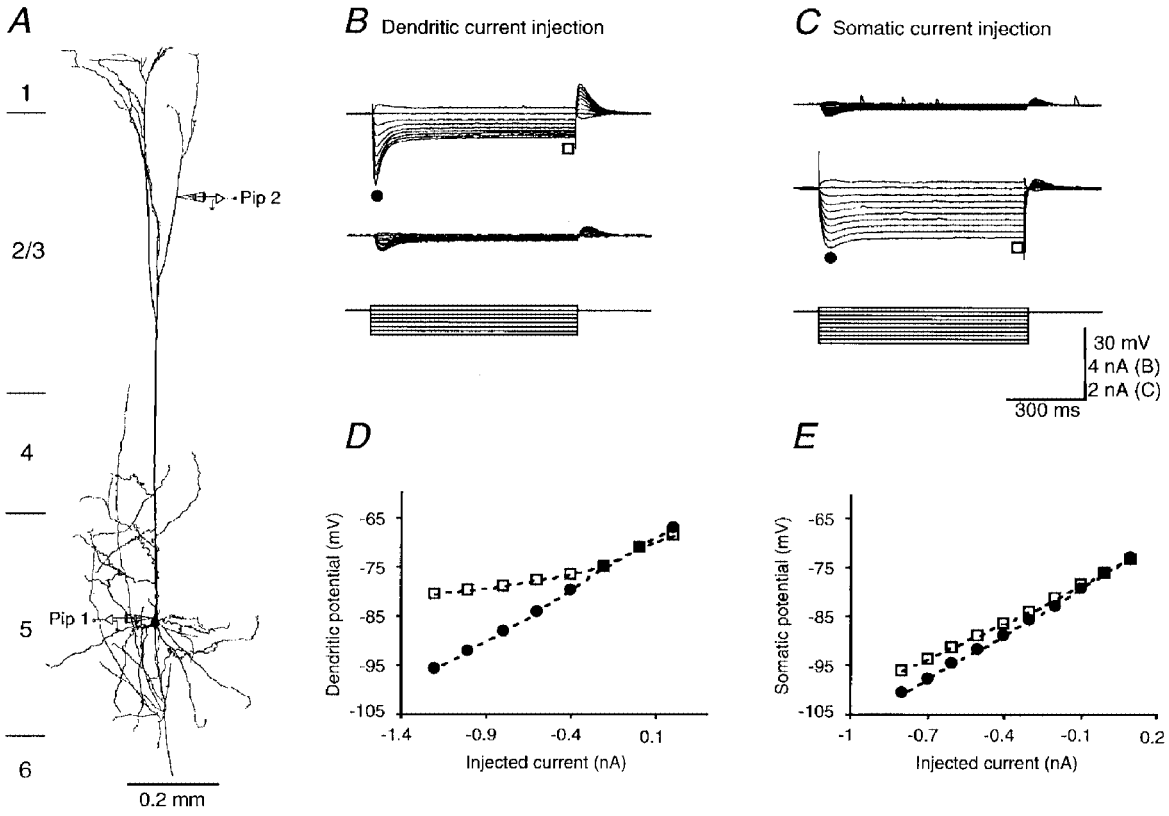

Figure 4. Membrane properties of a P42 pyramidal cell

A, morphology of a P42 pyramidal cell, reconstructed using Neurolucida. The schematic drawing of recording pipettes indicates the location of the dendritic (Pip 2, 941 μm distal from the soma) and somatic (Pip 1) recording. The length of the apical dendrite was 1303 μm. *B* and *C*, dendritic (upper traces) and somatic (middle traces) responses to step current injections (lower traces) into the tuft and the soma, respectively. The scale bars apply to *B* and *C*. *D* and *E*, early (● in *B* and *C*) and steady-state (□ in *B* and *C*) *I–V* relationships at the tuft and the soma, respectively. The resting membrane potential in the soma and dendrite was −76 and −71 mV, respectively. The input resistances at the soma and dendrite was 25 and 22 MΩ, respectively.

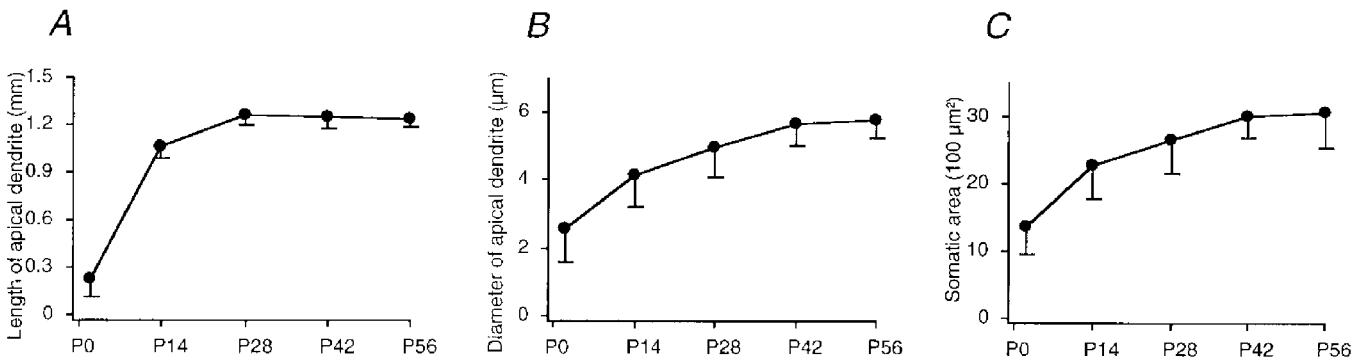

Figure 5. Morphological properties of apical dendrites and somata in the tufts at different stages of development

A, the length of the apical dendrite. *B*, the diameter of the apical dendrite. *C*, the somatic area.

with those of P14 cells ($P < 0{\cdot}01$). The basal dendrite and axon had similar appearances to those of P14 cells.

The difference in resting membrane potentials between the tuft and soma further increased, being $-69{\cdot}9 \pm 3{\cdot}4$ mV ($n = 33$) for the tuft and $-76{\cdot}6 \pm 2{\cdot}7$ mV ($n = 21$) for the soma. The input resistance continued to decrease, to $19{\cdot}4 \pm 4{\cdot}6$ ($n = 33$) and $35{\cdot}0 \pm 9{\cdot}5$ MΩ ($n = 21$) ($P < 0{\cdot}001$), respectively. In P28 cells, the depolarizing sag and inward rectification in the tuft were more obvious (Fig. 3*B–E*) and the electrotonic distance between the tuft and soma had increased as the attenuation of voltage responses between the tuft and soma increased to $76{\cdot}0 \pm 11{\cdot}0\%$ ($n = 8$; Fig. 3*B* and *C*).

P42 cortex. To follow the developmental change of layer 5 pyramidal cells to adulthood, we examined 11 neurons from P42 rats and recovered their morphology (Figs 4*A* and 10*A*). At P42 all neurons had a pyramidal soma, with a mean SA of $2921 \pm 323\ \mu m^2$ ($n = 11$), which was significantly larger

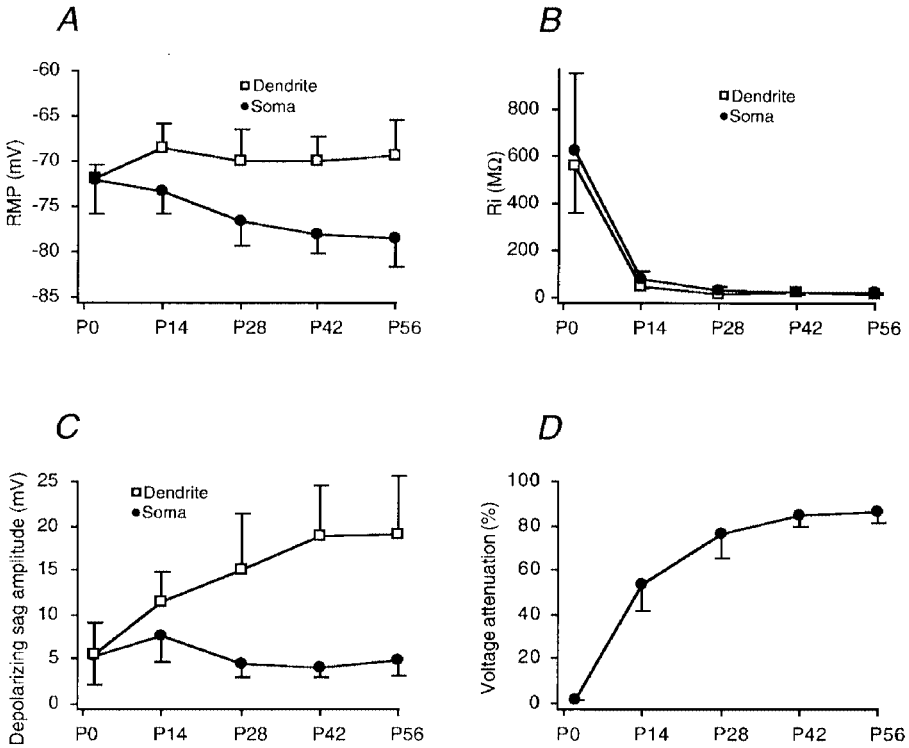

Figure 6. Physiological properties of dendritic tufts and somata at different stages of development

A, resting membrane potentials in the soma (●) and dendrite (□). *B*, input resistances in the soma and dendrite. *C*, amplitudes of depolarizing sag in the soma and dendrite. *D*, voltage attenuations between the soma and dendrite.

than that of P28 cells ($P < 0{\cdot}05$). The length of the apical dendrite was $1248 \pm 94\ \mu$m ($n = 11$), which is not significantly different from that in P28 cells ($P > 0{\cdot}05$). However, the diameter of the apical dendrite ($5{\cdot}5 \pm 0{\cdot}6\ \mu$m; $n = 11$) was significantly larger than P28 cells ($P < 0{\cdot}05$). The patterns of the basal dendrite and axon arbor were similar to those of P14 and P28 cells.

The resting membrane potentials in the tuft and soma were $-70{\cdot}0 \pm 2{\cdot}7$ ($n = 14$) and $-78{\cdot}0 \pm 2{\cdot}1$ mV ($n = 11$), respectively. The input resistance for the tuft ($20{\cdot}5 \pm 3{\cdot}1$ MΩ; $n = 14$) was slightly lower than that for the soma ($23{\cdot}5 \pm 3{\cdot}9$ MΩ; $n = 11$) in P42 cells ($P = 0{\cdot}046$). The depolarizing sag and inward rectification became prominent in the tuft, but not in the soma (Fig. 4). The dendritic tuft was more electrotonically isolated from the soma of P42 cells and the attenuation of voltage responses between the tuft and soma was $85{\cdot}0 \pm 5{\cdot}0$% ($n = 10$; Fig. 4*B* and *C*).

P56 cortex. Finally, we recorded from and recovered the morphology of nine pyramidal cells from P56 rats (Fig. 13*C*, left panel). These cells did not differ significantly in their morphological properties from P42 cells ($P > 0{\cdot}05$). The mean SA value, the length and diameter of the apical dendrite were $2970 \pm 514\ \mu$m^2 ($n = 9$), $1243 \pm 72\ \mu$m ($n = 9$) and $5{\cdot}6 \pm 0{\cdot}5\ \mu$m ($n = 9$), respectively. The basic membrane properties in P56 cells were also similar to those of P42 cells ($P > 0{\cdot}05$). The resting membrane potentials for the tuft and soma were $-69{\cdot}3 \pm 3{\cdot}9$ ($n = 9$) and $-78{\cdot}5 \pm 3{\cdot}3$ mV ($n = 9$), respectively, while the input resistances were $18{\cdot}2 \pm 5{\cdot}1$ ($n = 9$) and $22{\cdot}7 \pm 3{\cdot}3$ MΩ ($n = 9$), respectively. The attenuation of voltage responses between the tuft and soma was $86{\cdot}1 \pm 4{\cdot}6$% ($n = 7$).

Maturation of shape and membrane properties

In summary the changes in morphological and passive membrane properties suggest that the apical dendrite reaches its final length during the first 4 postnatal weeks (Fig. 5*A*), whereas the soma area and diameter of the apical dendrite continue to increase over the next 2 weeks (Fig. 5*B* and *C*). The membrane properties mature during the first 6 postnatal weeks. Initially, the resting membrane potentials

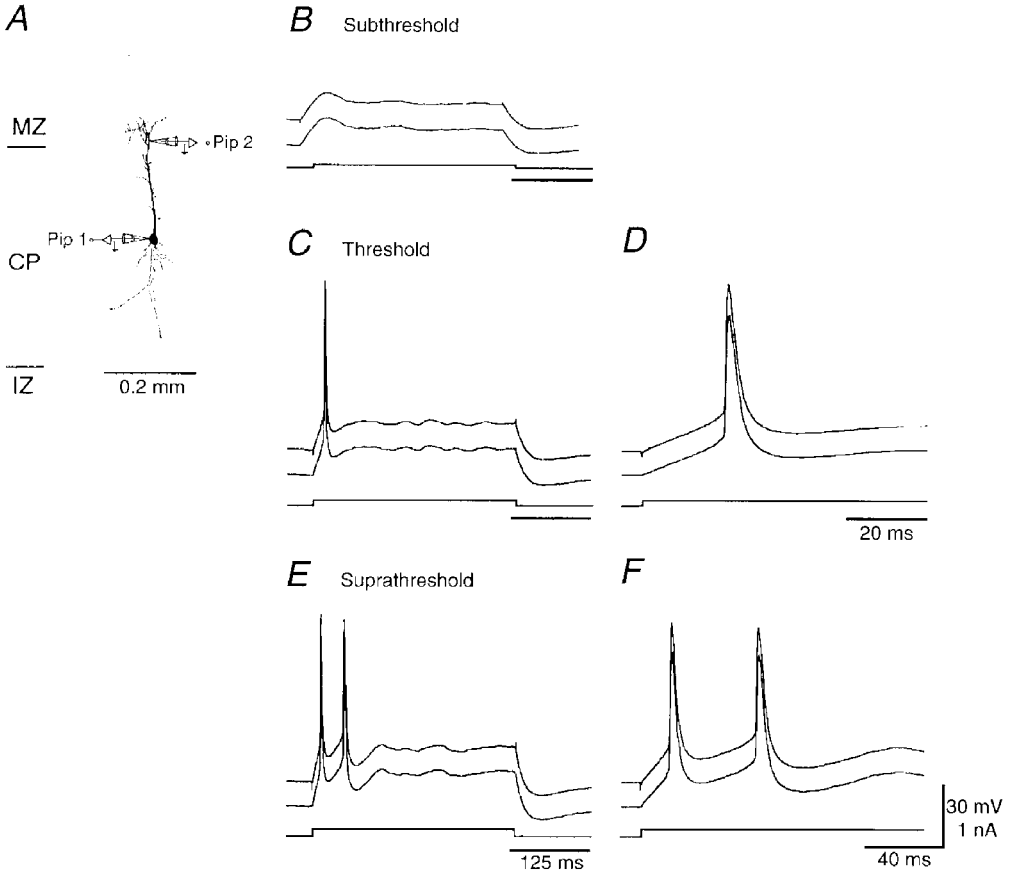

Figure 7. Regenerative potentials in the dendritic tuft of a P2 pyramidal cell

A, morphology of a P2 pyramidal cell, reconstructed using Neurolucida. The schematic drawing of recording pipettes indicates the location of the dendritic (Pip 2, 213 μm distal from the soma) and somatic (Pip 1) recordings. The length of the apical dendrite was 272 μm. *B*, *C* and *E*, dendritic and somatic responses to subthreshold, threshold and suprathreshold current injections into the tuft. *D* and *F*, the early responses in *C* and *E* are shown on a faster time scale. Regenerative potentials were generated simultaneously in the dendrite and soma. The resting membrane potential in the soma and dendrite was −80 and −70 mV, respectively.

are similar for the dendritic tuft and soma, then the dendrite becomes gradually less negative and the soma gradually more negative (Fig. 6*A*). The input resistances of both the tuft and soma drop rapidly during the first 2 postnatal weeks (Fig. 6*B*). In the following 4 weeks, they slowly reach their final low values. The sag amplitude in the tuft increases gradually in the first 6 postnatal weeks while that in the soma changes little (Fig. 6*C*). The attenuation of voltage responses between the tuft and soma increase gradually, reaching about 85% after the first 6 postnatal weeks (Fig. 6*D*).

Electrical excitability of dendritic tuft

P2 cortex. Injecting a depolarizing current step in the dendritic tuft of P2 pyramidal cells evoked brief all-or-none action potentials in both the soma and dendrite (Fig. 7). The threshold for the action potentials was $0{\cdot}05 \pm 0{\cdot}02$ nA, the voltage threshold was $-50{\cdot}7 \pm 5{\cdot}8$ mV. The dendritic and somatic potentials occurred at the same time and had a similar wave form (Fig. 7*D*), confirming electrotonic compactness of these neurons and their main regenerative conductance, a Na^+ conductance (see below), being uniformly distributed in the soma and dendrite (Huguenard *et al.* 1989). In response to a long suprathreshold current injection, these neurons typically fired a few action potentials at the onset of the current step but stopped long before the offset of the current step (Fig. 7*E* and *F*). The duration of the action potential in the tuft of P2 neurons, measured at the threshold, was $15{\cdot}5 \pm 11{\cdot}8$ ms.

P14 cortex. Injecting current in the P14 tufts also evoked all-or-none action potentials. The current threshold for the regenerative potentials was $0{\cdot}3 \pm 0{\cdot}1$ nA in these cells, the voltage threshold was $-48{\cdot}7 \pm 7{\cdot}6$ mV. At threshold, the dendritic regenerative potentials could be accompanied by single axonal action potentials (Fig. 8*C*). Figure 8*D* shows the dendritic and somatic regenerative potentials induced at threshold on an expanded time scale. The regenerative potential in the tuft had a longer duration and began earlier than the somatic action potential (Fig. 8*D*). The duration of

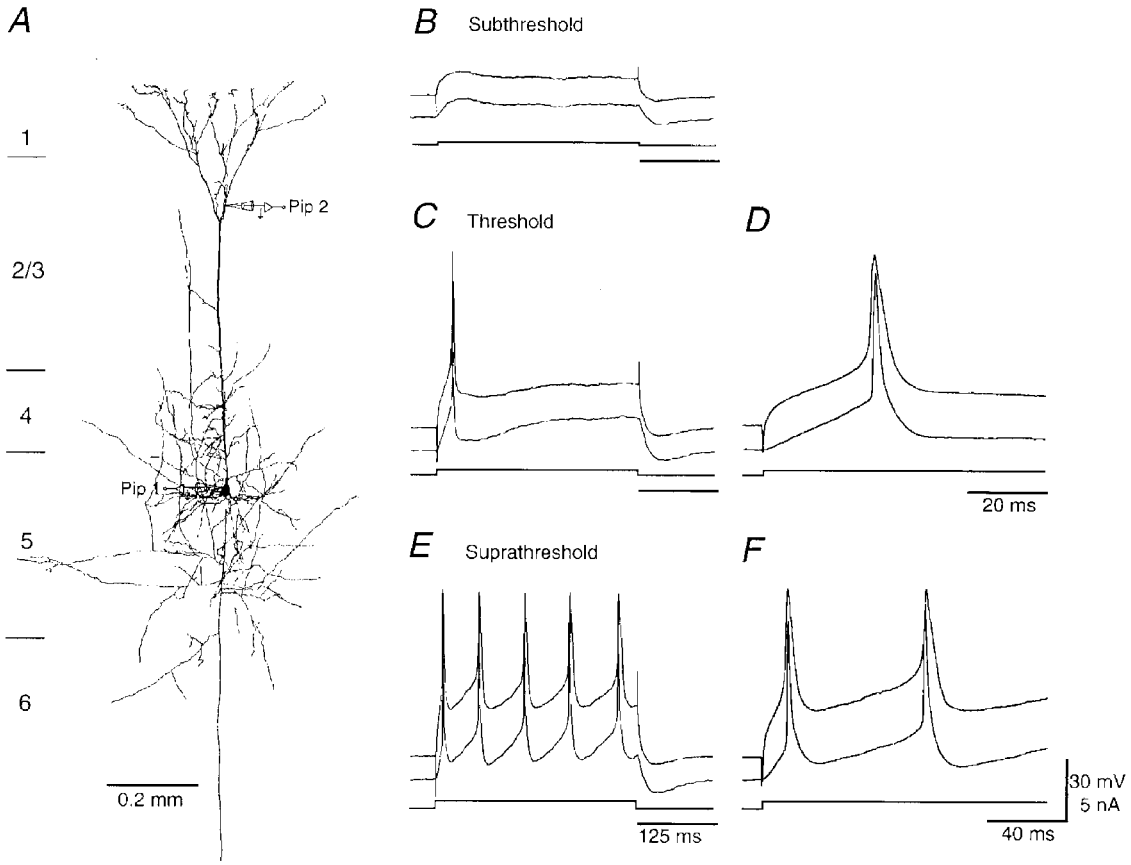

Figure 8. Regenerative potentials in the dendritic tuft of a P14 pyramidal cell

A, morphology of a P14 pyramidal cell, reconstructed using Neurolucida. The schematic drawing of recording pipettes indicates the location of the dendritic (Pip 2, 644 μm distal from the soma) and somatic (Pip 1) recordings. The length of the apical dendrite was 925 μm. *B*, *C* and *E*, dendritic and somatic responses to subthreshold, threshold and suprathreshold current injections into the tuft. *D* and *F*, the early responses in *C* and *E* are shown on a faster time scale. The first dendritic regenerative potential was generated earlier than the somatic one, whereas the second and the following somatic action potentials preceded the dendritic ones. The resting membrane potential in the soma and dendrite was −73 and −71 mV, respectively.

the regenerative potentials in the tuft was 8·7 ± 1·5 ms. A suprathreshold current injection evoked a train of action potentials (Fig. 8*E*). The first regenerative potential began earlier in the tuft than in the soma whereas the second and the following somatic action potentials preceded the dendritic ones (Fig. 8*F*).

Injecting a threshold depolarizing current at the dendritic trunk (ranging from 257 to 610 μm away from the soma) of P14 cells evoked a somatic action potential preceding the dendritic one ($n = 6$), consistent with our previous report (Stuart & Sakmann, 1994).

P28 cortex. The complex regenerative potentials evoked by long step depolarizations in the P28 tufts had a longer duration of 30·5 ± 7·2 ms (Fig. 9). The dendritic regenerative potentials could evoke axonal action potentials, eliciting either a single action potential or a burst of (2–3) action potentials in the soma (Fig. 9*C* and *D*). The current threshold for the regenerative potentials was 1·1 ± 0·4 nA in these cells and the voltage threshold was −50·2 ± 5·8 mV. Prolonged suprathreshold current injection could result in a maintained depolarization plateau in the dendrite and bursts of action potentials in the soma (Fig. 9*E*). The first regenerative potential began earlier in the tuft than in the soma whereas the second and the following somatic action potentials preceded the dendritic ones (Fig. 9*D* and *F*).

P42 and P52 cortex. The duration of the complex regenerative potentials was even longer in the P42 (Fig. 10) and P56 (not shown) tufts. The regenerative potential duration for these two groups of neurons was 56·3 ± 11·1 and 57·6 ± 9·9 ms, respectively. Dendritic regenerative potentials evoked by current pulse injections in both the P42 and P56 tufts always were concomitant by a burst of two to four action potentials in the soma (Fig. 10*C* and *D*, and 13*C*). The current thresholds for the regenerative potentials were 1·1 ± 0·2 and 1·1 ± 0·3 nA for P42 and P56 cells, respectively. The voltage thresholds were −47·3 ± 6·5

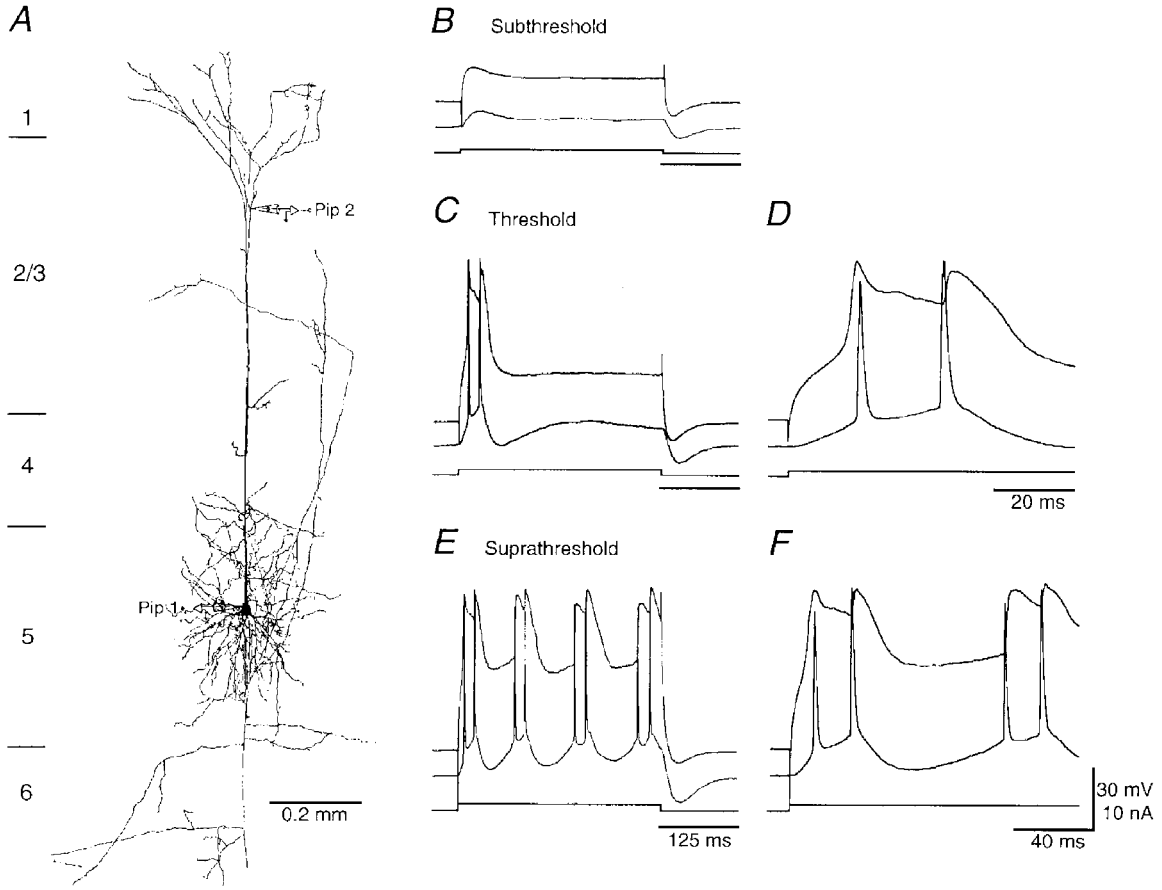

Figure 9. Regenerative potentials in the dendritic tuft of a P28 pyramidal cell

A, morphology of a P28 pyramidal cell, reconstructed using Neurolucida. The schematic drawing of recording pipettes indicates the location of the dendritic (Pip 2, 898 μm distal from the soma) and somatic (Pip 1) recordings. The length of the apical dendrite was 1250 μm. *B*, *C* and *E*, dendritic and somatic responses to subthreshold, threshold and suprathreshold current injections into the tuft. *D* and *F*, the early responses in *C* and *E* are showed in fast time scales. The first dendritic regenerative potential was generated earlier than the somatic one, whereas the second and the following somatic action potentials preceded the dendritic ones. The resting membrane potential in the soma and dendrite was −75 and −64 mV, respectively.

and $-48{\cdot}8 \pm 2{\cdot}6$ mV, respectively. Long suprathreshold current injection elicited a larger depolarization plateau in the P42 and P56 tufts than P28 ones (Fig. 10*E*). The first regenerative potential was recorded earlier in the tuft, whereas the subsequent action potentials were typically recorded first in the axon (Fig. 10*F*), presumably dependent upon the initiation of the axonal Na^+ action potentials (see also Fig. 11).

Pharmacology of dendritic regenerative potentials

The increasing duration of the regenerative potentials in the tuft dendrites suggests an increased contribution of the Ca^{2+} conductance (Schiller *et al.* 1997) and prolongation by back-propagated action potentials. We tested the contribution of the Ca^{2+} conductance by applying sodium and calcium channel blockers TTX, Ni^{2+} and Cd^{2+} (Fig. 11). TTX (1 μM) blocked somatic action potentials at all developmental ages. In the same experiments, TTX also blocked regenerative potentials in the P2 tufts ($n = 9$), but was progressively less effective on regenerative potentials in the P14 ($n = 6$), P28 ($n = 7$), P42 ($n = 9$), and P56 ($n = 5$; not shown) tufts. Adding 100 μM Ni^{2+} and 200 μM Cd^{2+} to the bath solution had no further effect in the P2 tufts ($n = 6$). However, it blocked the residual potentials substantially in the P14 ($n = 6$), P28 ($n = 6$), P42 ($n = 7$), and P56 ($n = 5$; not shown) tufts.

Dendritic electrical excitability during maturation

The active properties of tufts at different developmental stages are summarized in Fig. 12. The current intensity for evoking dendritic regenerative potentials by current injection (50 ms) increases during the first 4 postnatal weeks (Fig. 12*A*; $P < 0{\cdot}001$), and then remains constant (Fig. 12*A*; $P > 0{\cdot}05$). Because the voltage threshold changes very little, the increase in the current intensity is due mainly to the decrease in input resistance (Fig. 6). The

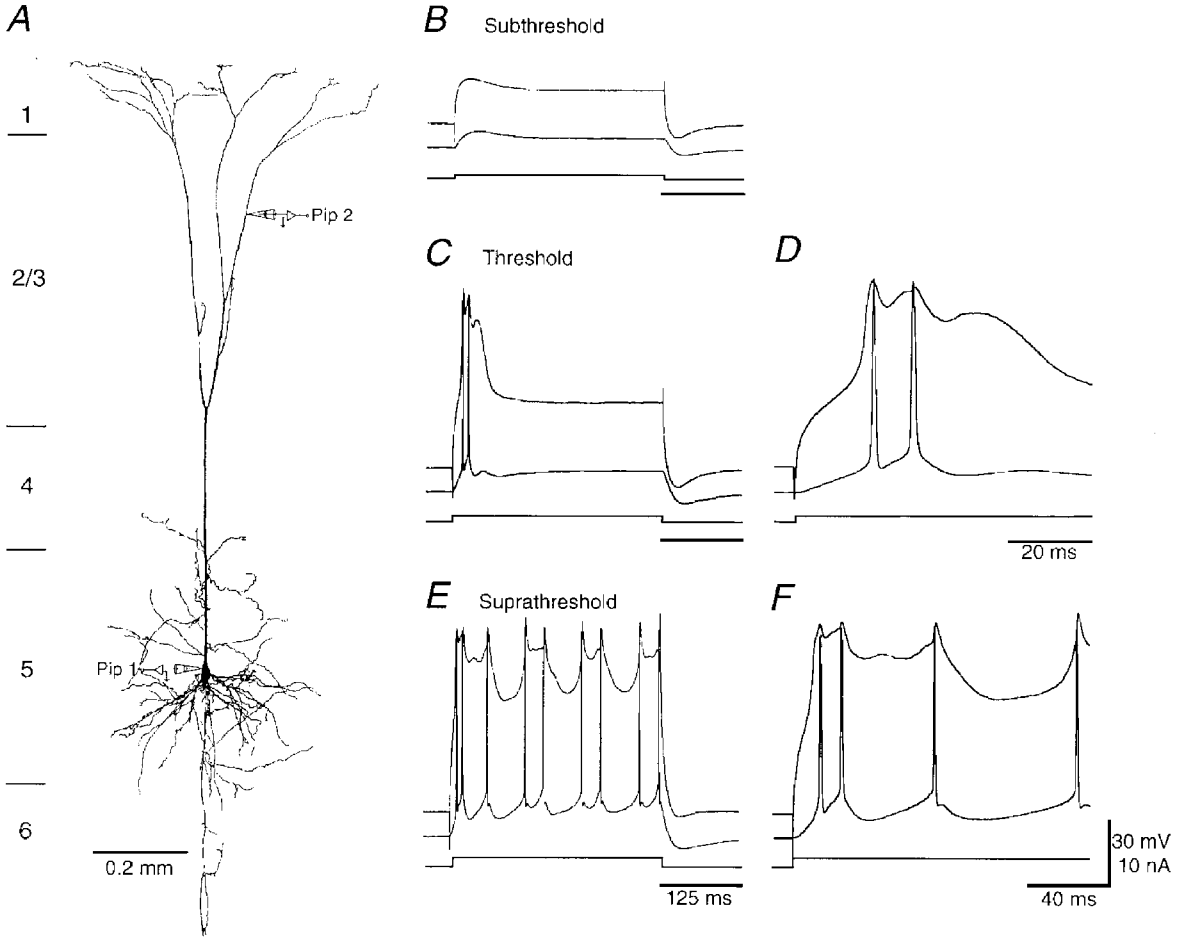

Figure 10. Regenerative potentials in the dendritic tuft of a P42 pyramidal cell

A, morphology of a P42 pyramidal cell, reconstructed using Neurolucida. The schematic drawing of recording pipettes indicates the location of the dendritic (Pip 2, 1002 μm distal from the soma) and somatic (Pip 1) recordings. The length of the apical dendrite was 1325 μm. *B*, *C* and *E*, dendritic and somatic responses to subthreshold, threshold and suprathreshold current injections into the tuft. *D* and *F*, the early responses in *C* and *E* are showed in fast time scales. The first dendritic regenerative potential was generated earlier than the somatic ones, whereas the second and the following somatic action potentials usually preceded the dendritic ones. The resting membrane potential in the soma and dendrite was -81 and -72 mV, respectively.

duration of the dendritic regenerative potentials decreases somewhat initially during the first 2 postnatal weeks and then increases in the following 4 weeks. The amplitude of regenerative potentials also increases slightly during development (Fig. 12*C*). The largest change occurs in the ionic dependence of the regenerative potentials, switching from being mainly Na^+ dependent to mainly Ca^{2+} dependent (Fig. 12*C*). Finally, the reliability of the coupling between dendritic and axonal action potential initiation zones, measured by rectangular current injections, initially decreases between P14 and P28 and then increases again in > P42 rats (Fig. 12*D*; see also results below).

Coupling of dendritic and axonal action potential initiation sites during maturation

The maturation of the electrical excitability of dendritic tufts is expected to affect forward signalling of apical inputs and backward signalling of basal inputs along the main apical dendrite. We attempted to delineate changes of signalling of distal dendritic inputs to the soma by current injection into the dendritic tuft and by selective layer 1 stimulation.

We first examined the effects of the regenerative potentials in the tuft evoked by injecting a depolarizing current at threshold intensity and measured the shape and time of occurrence of the regenerative potentials at the soma and dendrite (Fig. 13). At P2 regenerative potentials were recorded almost simultaneously in the tuft and soma. At P14 and P28 the regenerative potentials in about half the tufts (4 of 7 cells at P14, Fig. 13*A*; 9 of 19 cells at P28) were not accompanied by somatic action potentials (Fig. 13*B*). Suprathreshold current injections did, on the other hand, frequently, but not always, elicit somatic action potentials (see also Schiller *et al.* 1997). In the tufts of the adult cortex (20 of 20 cells, P42 and P56), current injections in the tuft evoked a complex regenerative potential in the tuft and one to four action potentials in the soma (Fig. 13*C*). When a larger sample of cells were examined, however, we did observe a small population of adult neurons generating isolated dendritic regenerative potentials (2 of 56 cells; authors' unpublished data). In older animals, the dendritic recordings were often made more distally to the soma and the electrotonic attenuation of steady-state signals was larger. Therefore the higher probability with which

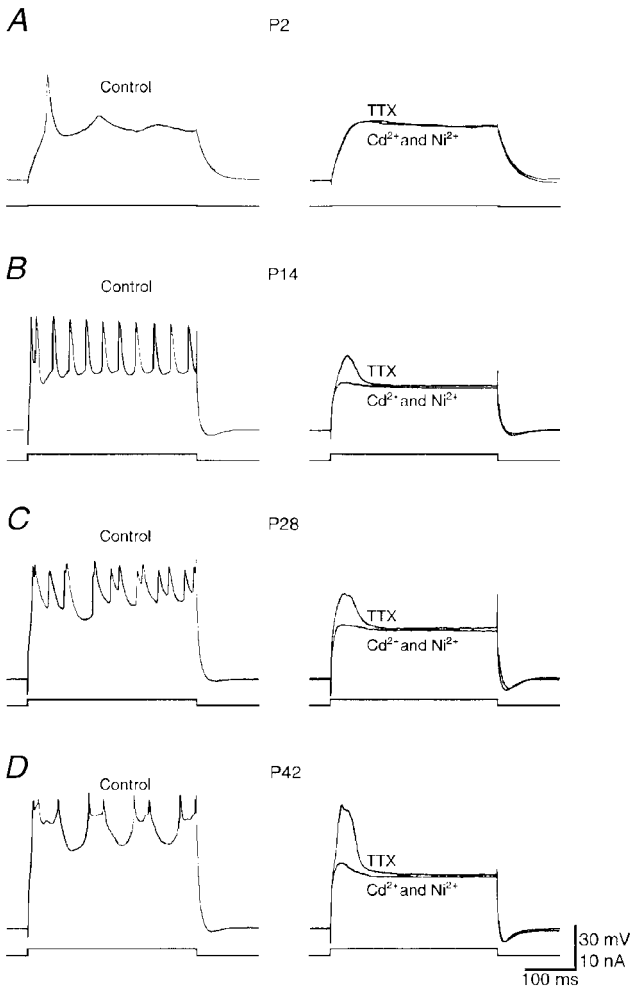

Figure 11. Regenerative potentials in the dendritic tufts of P2 (*A*), P14 (*B*), P28 (*C*) and P42 (*D*) cells

Left traces are the dendritic responses to a suprathreshold current injection in the dendrites (somatic recordings are not shown). Right traces are the responses with 1 μM TTX included in the bath solution, and responses after adding 200 μM Cd^{2+} and 100 μM Ni^{2+} to the bath solution. The resting membrane potential of the soma of these four cells was −68, −73, −72 and −81 mV, respectively. The resting membrane potential in the tufts was −71, −71, −71 and −72 mV, respectively.

threshold current injection into the dendritic tuft evoked both dendritic and somatic action potentials was not due to a shorter electrotonic distance between the site of current injection and the axon. Rather this reflects the fact that more regenerative conductances are activated by dendritic current injection.

The dendritic regenerative potentials and the concomitant somatic action potential pattern evoked by layer 1 stimulation in slices which had a longitudinal cut also changed with development (Fig. 14). Stimulation of the distal layer 1 synaptic inputs could evoke regenerative potentials in the tuft of both young and adult neurons. For P14 (4 of 4 cells) and P28 cells (3 of 4 cells), the regenerative potential at threshold stimulation remained localized to the dendrite (Fig. 14*B* and *E*). Suprathreshold stimulation did, in some neurons, evoke somatic action potentials. In contrast, in P42 and P56 cells ($n = 8$), threshold stimulation elicited a complex regenerative potential in the tuft and concomitantly a single action potential or, more frequently, with a burst of two to three action potentials in the soma (Fig. 14*C–E*). The pattern of somatic action potentials changed with stimulus strength. The number of somatic action potentials could either increase or decrease with increasing stimulus strength. In addition, the sequence of dendritic and somatic action potentials could vary. At threshold the first somatic action potential could either precede (2 of 8 cells) or follow (6 of 8 cells) the dendritic regenerative potential. The following somatic action potentials (i.e. the second and third action potential) always preceded the respective peaks of the dendritic complex regenerative potential, suggesting that back-propagating axonal action potentials might further broaden the dendritic complex potential.

DISCUSSION

The results show that young layer 5 pyramidal cells have many properties of mature cells after the 2nd postnatal week (P14). The apical dendrite of pyramidal cells is, however, not fully mature until the end of 6th postnatal week (P42). The dendritic tuft switches from being electrotonically close to the soma to being isolated from it. Concomitantly, the ionic dependence of the regenerative potentials in the dendritic tuft switches from being mainly Na^+ dependent to Na^+ and Ca^{2+} dependent. In the juvenile cortex (P28), the regenerative dendritic potentials are still relatively short and often fail to initiate axonal action potentials. In contrast, in adult neurons (> P42), the regenerative potentials in the tuft are frequently accompanied by one or more somatic action potentials initiated in the axon. The interaction of dendritic and axonal active conductances gives rise to 'complex' dendritic potentials, independent of the intrinsic action potential

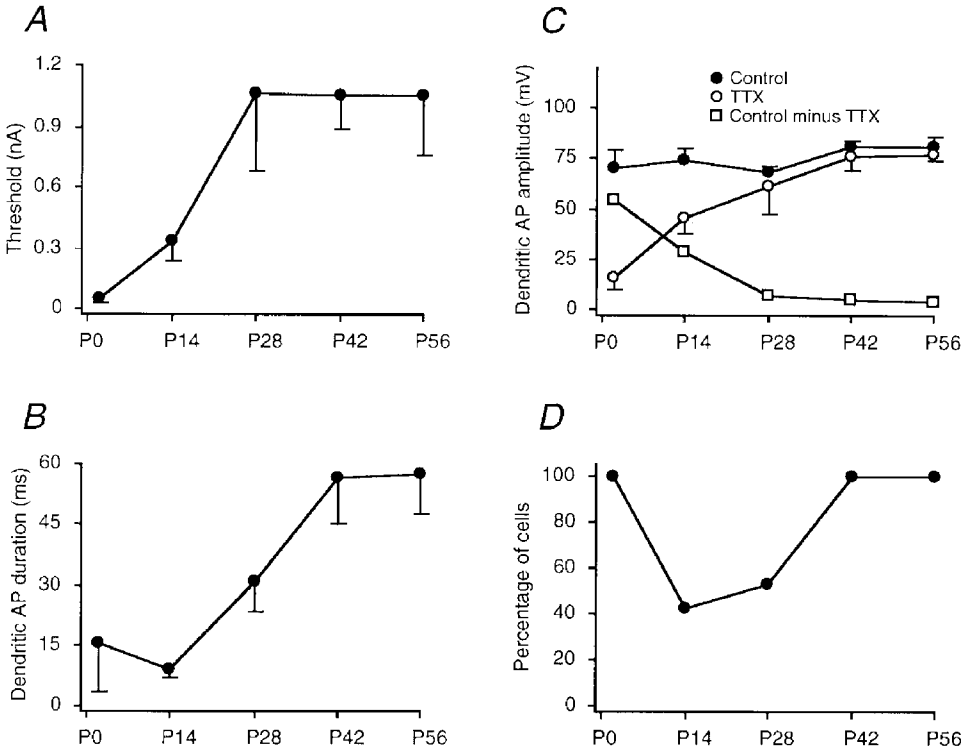

Figure 12. Properties of regenerative potentials in the tufts at different stages of development

A, the threshold of dendritic regenerative potentials. *B*, the duration of dendritic regenerative potentials. *C*, the amplitude of dendritic regenerative potentials in the normal bath solution, in the 1 μM TTX solution, and their differences. *D*, percentage of cells which responded to the threshold current injections in the tufts with somatic firing at different developmental stages.

patterns in the soma (i.e. regular-spiking *vs.* burst-spiking; see Connors & Gutnick, 1990).

Morphological maturation and passive electrical properties

The morphological properties of pyramidal cells mature within the first 6 postnatal weeks, consistent with the previous anatomical findings (Petit *et al.* 1988; Kasper *et al.* 1994). The development of the electrophysiological properties in the soma has been examined previously using the sharp electrode recording technique (McCormick & Prince, 1987; Franceschetti *et al.* 1998). Using whole-cell voltage recording with patch pipettes, we found a considerably higher input resistance and a significantly more negative resting membrane potential in the soma of young pyramidal neurons (557 *vs.* 150 MΩ, respectively; see also Kim *et al.* 1995). These differences probably result from the fact that sharp intracellular electrodes used previously may introduce a non-selective leak, particularly in the small neurons of young animals (Staley *et al.* 1992). By recording directly from the dendritic tuft of layer 5 pyramidal neurons, we revealed that the input resistance in the tuft

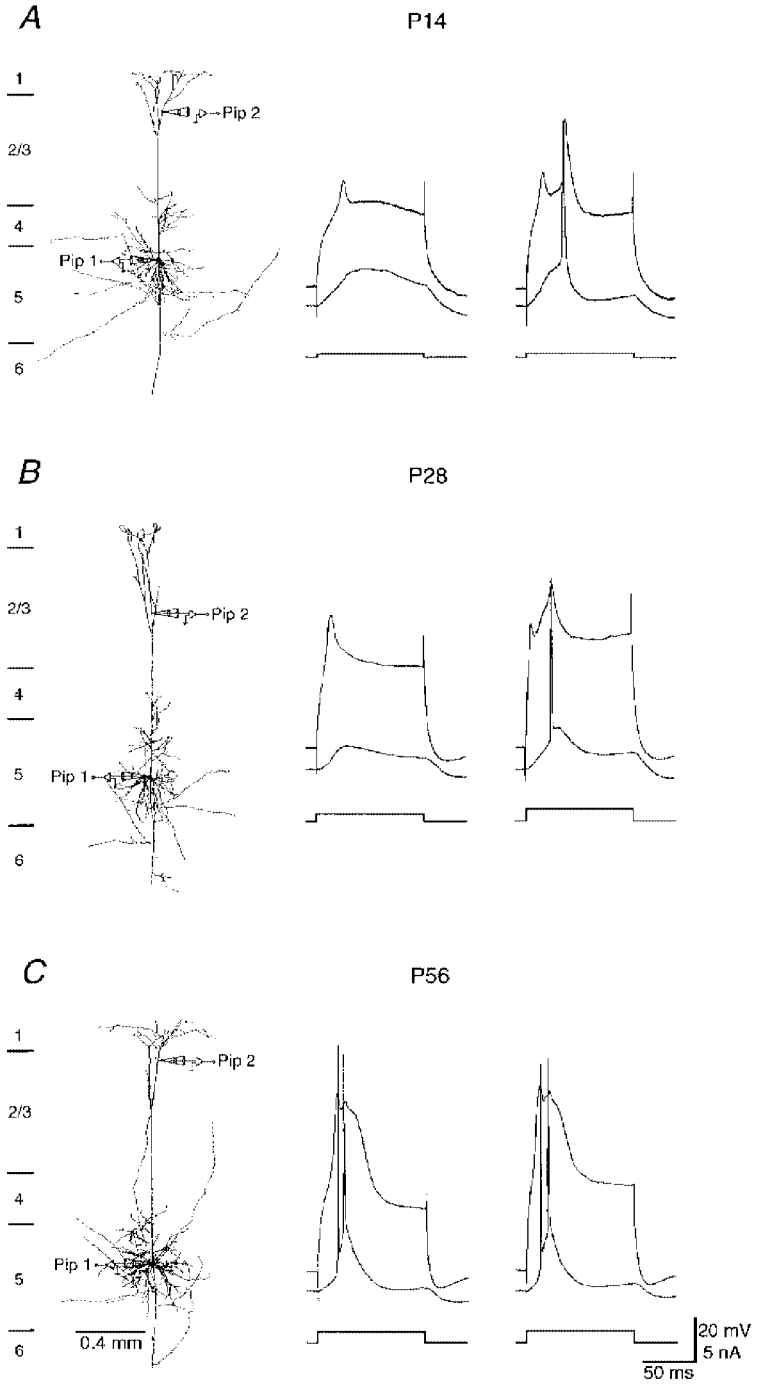

Figure 13. Effects of current injection-evoked regenerative potentials in the apical tuft on somatic firing at different stages of development

Threshold current injection into dendritic tuft induced only subthreshold responses in the soma of a P14 cell (*A*, left-hand traces) and a P28 cell (*B*, left-hand traces), but a burst of sodium action potentials in the soma of a P56 cell (*C*, left-hand recordingtraces). Supra-threshold current injection into dendritic tufts induced suprathreshold responses in the soma of all three cells (*A–C*, right-hand traces). The morphology of three cells is shown to the left in *A–C*. The dendritic recordings were located at 868, 988 and 1221 μm away from the soma, respectively. The length of the apical dendrite of these cells was 1117, 1514 and 1443 μm, respectively. The scale bars apply to *A–C*. The resting membrane potential in the soma of these three cells was −74, −77 and −74 mV, respectively. The resting membrane potential in the tufts was −66, −62 and −64 mV, respectively.

decreases during development, similar to the soma. The large decrease in the input resistance may result from the increasing expression of the conductances that open at the resting membrane potential in layer 5 pyramidal neurons (e.g. I_h, I_M and other potassium conductances; see Hamill *et al.* 1991; Kang *et al.* 1996; Zhu *et al.* 1999).

Our results also indicate that neonatal (P2) pyramidal cells are electrotonically compact because the voltage responses at the soma and tuft are comparable. In contrast, in adult (> P42) pyramidal cells, the dendritic tuft is electrotonically isolated from the soma and axon. This difference appears to result from the alterations in both morphological and physiological properties since both properties change significantly during development. In addition, there is also an intriguing change in resting membrane potential in the soma and the tuft during development. Instead of becoming more hyperpolarized like the soma, the resting membrane potential in the tuft becomes more depolarized. Thus, a prominent potential difference between the soma and the tuft is gradually established during postnatal development. The potential difference probably results from two changes that occur during development. First, there is an increase in electrotonic isolation between the soma and the tuft, which makes the potential difference possible. Second, selectively expressing more depolarizing I_h in the tuft (this study) and more hyperpolarizing potassium conductances in the soma (Kang *et al.* 1996) charges the potential difference.

Active membrane properties during maturation

The soma of layer 5 pyramidal cells can generate action potentials at all developmental stages (McCormick & Prince, 1987; Kim *et al.* 1995; Franceschetti *et al.* 1998). The dendritic tuft of layer 5 pyramidal cells also supports the regenerative potential at all developmental stages, indicating that active conductances in the dendrite are expressed at all stages. The duration of the regenerative potentials evoked by current injection in the tuft increases during development, presumably reflecting an increased contribution of Ca^{2+} conductance. At P14 the duration of dendritic regenerative potentials is slightly shorter than at P2, most probably resulting from a rapid increase in K^+ conductance during the first 2 postnatal weeks (Hamill *et al.* 1991; Kang *et al.* 1996).

The dendritic regenerative potentials switch from being mainly Na^+ dependent to being dependent on both Na^+ and Ca^{2+} during development. Their voltage threshold remains

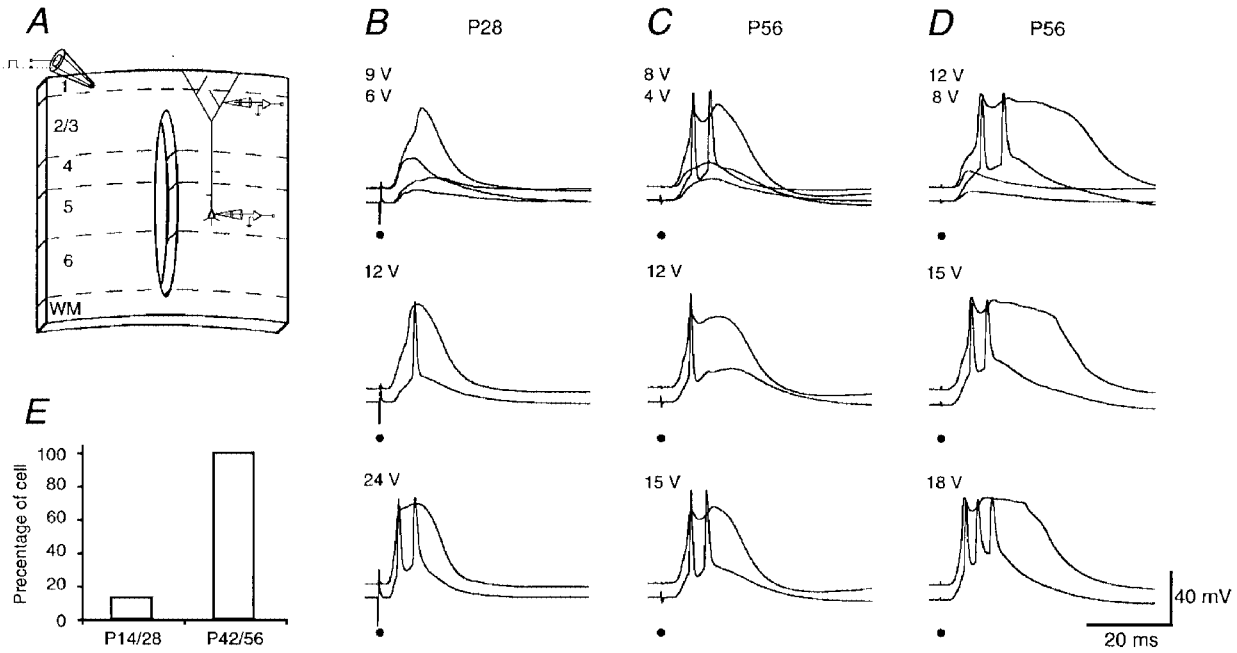

Figure 14. Effects of layer 1 stimulation-evoked regenerative potentials in the apical tuft on somatic firing at different stages of development

A, a schematic drawing of the preparation used to selectively stimulate layer 1 input. *B–D*, threshold layer 1 stimulations for the regenerative potentials in the tuft induced only subthreshold responses in the soma of a P28 cell, but suprathreshold responses in the soma of two P56 cells (upper traces). Suprathreshold stimulations induced one to three action potentials in the somata (middle and upper recording traces). The dendritic recordings were located at primary tufts 748, 731 and 788 μm away from the soma. The length of the apical dendrite of these cells was 1186, 1316 and 1207 μm, respectively. The scale bars apply to *B–D*. The resting membrane potential in the soma of these cells was −78, −84 and −78 mV, respectively. The resting membrane potential in the tufts was −70, −74 and −72 mV, respectively. *E* shows the percentage of young (left) and adult (right) cells which responded to the threshold layer 1 stimulation for the regenerative potentials in the tufts with somatic firing.

quite constant at a low value. On the other hand, the intensity of depolarizing current needed for evoking regenerative potentials in the tuft of older animals increases due to the reduced input resistance. In adult tufts, the average threshold intensity for action potentials is about 1·1 nA, higher than the soma (0·7 nA).

In adult cells, Ca^{2+} channels mediate a substantial part of the regenerative potentials in the tuft. The contribution of Na^+ channels in these potentials is relatively small and is typically 'masked' by the large Ca^{2+}-dependent potentials. Clearly, this does not imply that Na^+ channel density in the dendritic tuft decreases during development since the input resistance of the tuft drops sharply in the same period and a much smaller depolarization will result from the activation of the same number of Na^+ channels. Because the density of K^+ channels in neocortical pyramidal neurons increases during development (Hamill *et al.* 1991; Kang *et al.* 1996), the broadening of Na^+- and Ca^{2+}-dependent regenerative potentials in the tuft implies a substantial increase in Ca^{2+} channel density in the tuft during the postnatal development. At P42, the regenerative potentials in the tuft reach their final amplitude and duration, suggesting that Ca^{2+} channels may have reached their peak density. The developmental increase in the density of Ca^{2+} channels in the apical dendrite thus parallels a similar increase of Ca^{2+} currents in the soma of cortical cells (Lorenzon & Foehring, 1995).

Using a brief EPSC waveform injection, a small locally restricted regenerative potential can be isolated in the tuft (our unpublished data). The potential is mainly Na^+ dependent, due presumably to the decoupling of the activation of Na^+ and Ca^{2+} conductances and failure of generating the complex dendritic potential. This suggests that Na^+ conductance is essential in initiating the tuft regenerative potentials at low threshold. In addition, T- and R- type Ca^{2+} channels are present in the apical dendrite and have a relatively low threshold for activation (Magee & Johnston, 1995; Markram *et al.* 1995; Kavalali *et al.* 1997). These conductances may help to lower the threshold of the dendritic regenerative potentials. Because these Ca^{2+} and Na^+ channels show prolonged inactivation (Kavalali *et al.* 1997; Colbert *et al.* 1997; Jung *et al.* 1997), they may account for the long refractory period of the dendritic regenerative potentials (our unpublished data; Chang, 1951). N- and P-/Q- channels are the main types of Ca^{2+} channels present in the dendrite (Kavalali *et al.* 1997). Since these channels inactivate slowly, they may contribute to the prolonged time course of the distal regenerative potentials.

Functional significance of layer 5 pyramid maturation

In addition to the layer 4 inputs received at the basal dendrites, the distal apical dendrites of layer 5 pyramidal neurons are densely innervated by the layer 1 inputs, coming from the cortical feedback and ascending regulatory neural systems (e.g. Herkenham, 1980; Delima & Singer, 1986; Zeki & Shipp, 1988). They may contribute to complex behaviour such as attention and perception (Cauller & Kulics, 1988; Squire & Zola-Morgan, 1991). Previous studies have shown that the regenerative conductances in the apical dendritic trunk can amplify the distal synaptic inputs in pyramidal cells (Kim & Connors, 1993; Magee & Johnston, 1995; Schwindt & Crill, 1995; Gillessen & Alzheimer, 1997). When these tuft conductances are activated, for example by synaptic inputs *in vitro* (Schiller *et al.* 1997) or natural stimuli *in vivo* (Zhu & Connors, 1999), a regenerative dendritic potential is generated which integrates synaptic inputs locally. Therefore, the very distal synaptic inputs can be amplified as early as the signals reach the dendritic arbor.

In this study, we showed that the long dendritic trunk and low input resistance make the tuft dendrite of adult layer 5 pyramidal cells not only distally located, but also electrotonically isolated from the basal dendrite, soma and axon. Correspondingly, in adult pyramidal neurons, large, suprathreshold synaptic inputs from layer 1 can be non-linearly amplified and can trigger axonal action potentials. In contrast, small synaptic inputs, without being amplified by the dendritic regenerative potentials, give only very small depolarizations in the soma. Thus, the isolated distal tuft, capable of generating the dendritic regenerative potentials, can boost selectively the salient distal inputs.

The distal action potential initiation zone can interplay with the axonal action potential initiation zone. This makes the dynamic interactions between the distal and proximal synaptic inputs possible. Indeed, our recent study has shown that coincident apical and basal inputs enhance the axon's ability to detect and amplify the small distal dendritic inputs (Larkum *et al.* 1999). Namely, the axon initiation site can generate a burst of action potentials when a subthreshold distal dendritic input and a suprathreshold basal dendritic input occur within a short time window of a few milliseconds.

Conclusions

During the early developmental period ($\leqslant$P14), new synapses form and mature rapidly at the dendritic arbor of pyramidal cells (Miller & Peters, 1981; Harris *et al.* 1992; see also Isaac *et al.* 1997). The relative electrotonic compactness, as well as the reliable back-propagating action potentials (Stuart & Sakmann, 1994), may be important for the dendrite to modulate synaptic efficacy according to the cells' input and output patterns (Markram *et al.* 1997). At the later stages, when most cortical synapses have been formed ($>$P28), the tuft dendrite becomes electrotonically isolated from the soma. The development of the slow and Na^+- and Ca^{2+}-dependent regenerative potentials in the adult tuft may be crucial for its mature functions. For example, the Ca^{2+} action potentials are important for detecting the salient distal synaptic inputs and bridging the electrotonic distance between the tuft dendrite and soma. In addition, they are involved in detecting the coincident synaptic inputs arriving at the apical and basal dendritic arbors (Larkum *et al.* 1999). Finally, the slow time course

allows the Ca^{2+} action potentials to enhance the efficiency of the salient distal inputs and coincident inputs by promoting burst firing, which increases the reliability of the synaptic transmission between layer 5 pyramidal neurons and their target cells (Lisman, 1997, Williams & Stuart, 1999).

Amitai, Y., Friedman, A., Connors, B. W. & Gutnick, M. J. (1993). Regenerative activity in apical dendrites of pyramidal cells in neocortex. *Cerebral Cortex* **3**, 26–38.

Berry, M. & Rogers, A. W. (1965). The migration of neuroblasts in the developing cerebral cortex. *Journal of Anatomy* **99**, 691–709.

Cauller, L. J., Clancy, B. & Connors, B. W. (1998). Backward cortical projections to primary somatosensory cortex in rats extend long horizontal axons in layer I. *Journal of Comparative Neurology* **390**, 297–310.

Cauller, L. J. & Connors, B. W. (1994). Synaptic physiology of horizontal afferents to layer I in slices of rat SI neocortex. *Journal of Neuroscience* **14**, 751–762.

Cauller, L. J. & Kulics, A. T. (1988). A comparison of awake and sleeping cortical states by analysis of the somatosensory-evoked response of postcentral area 1 in rhesus monkey. *Experimental Brain Research* **72**, 584–592.

Chang, H.-T. (1951). Changes in excitability of cerebral cortex following single electric shock applied to cortical surface. *Journal of Neurophysiology* **14**, 95–111.

Chang, H.-T. (1952). Cortical and spinal neurons: cortical neurons with particular reference to the apical dendrites. *Cold Spring Harbor Symposium of Quantitative Biology* **17**, 189–202.

Colbert, C. M., Magee, J. C., Hoffman, D. A. & Johnston, D. (1997). Slow recovery from inactivation of Na^+ channels underlies the activity-dependent attenuation of dendritic action potentials in hippocampal CA1 pyramidal neurons. *Journal of Neuroscience* **17**, 6512–6521.

Connors, B. W. & Gutnick, M. J. (1990). Intrinsic firing patterns of diverse neocortical neurons. *Trends in Neuroscience* **13**, 99–104.

De Lima, A. D. & Singer, W. (1986). Cholinergic innervation of the cat striate cortex: a choline acetyltransferase immunocytochemical analysis. *Journal of Comparative Neurology* **250**, 324–338.

Franceschetti, S., Sancini, G., Panzica, F., Radici, C. & Avanzini, G. (1998). Postnatal differentiation of firing properties and morphological characteristics in layer 5 pyramidal neurons of the sensorimotor cortex. *Neuroscience* **83**, 1013–1024.

Gillessen, T. & Alzheimer, C. (1997). Amplification of EPSPs by low Ni^{2+}- and amiloride-sensitive Ca^{2+} channels in apical dendrites of rat CA1 pyramidal neurons. *Journal of Neurophysiology* **77**, 1639–1643.

Hamill, O. P., Huguenard, J. R. & Prince, D. A. (1991). Patch-clamp studies of voltage-gated currents in identified neurons of the rat cerebral cortex. *Cerebral Cortex* **1**, 48–61.

Harris, K. M., Jensen, F. E. & Tsao, B. (1992). Three-dimensional structure of dendritic spines and synapses in rat hippocampus (CA1) at postnatal day 15 and adult ages: implications for the maturation of synaptic physiology and long-term potentiation. *Journal of Neuroscience* **12**, 2685–2705.

Herkenham, M. (1980). Laminar organization of thalamic projections to the rat neocortex. *Science* **207**, 532–535.

Huguenard, J. R., Hamill, O. P. & Prince, D. A. (1989). Sodium channels in dendrites of rat cortical pyramidal neurons. *Proceedings of the National Academy of Sciences of the USA* **86**, 2473–2477.

Isaac, J. T. R., Crair, M. C., Nicoll, R. A. & Malenka, R. C. (1997). Silent synapses during developmental of thalamocortical inputs. *Neuron* **18**, 269–280.

Johnson, R. R. & Burkhalter, A. (1997). A polysynaptic feedback circuit in rat visual cortex *Journal of Neuroscience* **17**, 7129–7140.

Jones, E. G. (1998). Viewpoint – the core and matrix of thalamic organization. *Neuroscience* **85**, 331–345.

Jones, E. G. & Powell, T. P. (1970). Electron microscopy of the somatic sensory cortex of the cat. II. The fine structure of layers I and II. *Philosophical Transactions of the Royal Society of London* B **257**, 13–21.

Jung, H. Y., Mickus, T. & Spruston, N. (1997). Prolonged sodium channel inactivation contributes to dendritic action potential attenuation in hippocampal pyramidal neurons. *Journal of Neuroscience* **17**, 6639–6646.

Kang, J., Huguenard, J. R. & Prince, D. A. (1996). Development of BK channels in neocortical pyramidal neurons. *Journal of Neurophysiology* **76**, 188–198.

Kasper, E. M., Lubke, J., Larkman, A. U. & Blakemore, C. (1994). Pyramidal neurons in layer 5 of the rat visual cortex. III. Differential maturation of axon targeting, dendritic morphology, and electrophysiological properties. *Journal of Comparative Neurology* **339**, 495–518.

Kavalali, E. T., Zhuo, M., Bito, H. & Tsien, R. W. (1997). Dendritic Ca^{2+} channels characterized by recordings from isolated hippocampal dendritic segments. *Neuron* **18**, 651–663.

Kim, H. G. & Connors, B. W. (1993). Apical dendrites of the neocortex: correlation between sodium- and calcium-dependent spiking and pyramidal cell morphology. *Journal of Neuroscience* **13**, 5301–5311.

Kim, H. G., Fox, K. & Connors, B. W. (1995). Properties of excitatory synaptic events in neurons of primary somatosensory cortex of neonatal rats. *Cerebral Cortex* **5**, 148–157.

Larkum, M. E., Zhu, J. J. & Sakmann, B. (1999). A new cellular mechanism for coupling inputs arriving at different cortical layers. *Nature* **398**, 338–341.

Lisman, J. E. (1997). Burst as a unit of neural information: making unreliable synapses reliable. *Trends in Neurosciences* **20**, 38–43.

Lorenzon, N. M. & Foehring, R. C. (1995). Characterization of pharmacologically identified voltage-gated calcium channel currents in acutely isolated rat neocortical neurons. II. Postnatal development. *Journal of Neurophysiology* **73**, 1443–1451.

Lysakowski, A., Wainer, B. H., Rye, D. B., Bruce, G. & Hersh, L. B. (1986). Cholinergic innervation displays strikingly different laminar preferences in several cortical areas. *Neuroscience Letter* **64**, 102–108.

McCormick, D. A. & Prince, D. A. (1986). Mechanisms of action of acetylcholine in the guinea-pig cerebral cortex *in vitro*. *Journal of Physiology* **375**, 169–194.

McCormick, D. A. & Prince, D. A. (1987). Post-natal development of electrophysiological properties of rat cerebral cortical pyramidal neurons. *Journal of Physiology* **393**, 743–762.

Magee, J. C. & Johnston, D. (1995). Characterization of single voltage-gated Na^+ and Ca^{2+} channels in apical dendrites of rat CA1 pyramidal neurons. *Journal of Physiology* **487**, 67–90.

Markram, H., Helm, P. J. & Sakmann, B. (1995). Dendritic calcium transients evoked by single back-propagating action potentials in rat neocortical pyramidal neurons. *Journal of Physiology* **485**, 1–20.

Markram, H., Lübke, J., Frotscher, M. & Sakmann, B. (1997). Regulation of synaptic efficacy by coincidence of postsynaptic APs and EPSPs. *Science* **275**, 213–215

Miller, M. & Peters, A. (1981). Maturation of rat visual cortex. II. A combined Golgi-electron microscope study of pyramidal neurons. *Journal of Comparative Neurology* **203**, 555–573.

Petit, T. L., LeBoutillier, J. C., Gregorio, A. & Libstug, H. (1988). The pattern of dendritic developement in the cerebral cortex of the rat. *Developmental Brain Research* **41**, 209–219.

Regehr, W., Kohoe, J., Ascher, P. & Armstrong, C. (1993). Synpatically triggered action potentials in dendrites. *Neuron* **11**, 145–151.

Reyes, A. & Sakmann, B. (1999). Developmental switch in the short-term modification of unitary EPSPs evoked in layer 2/3 and layer 5 pyramidal neurons of rat neocortex. *Journal of Neuroscience* **19**, 3827–3835.

Schiller, J., Schiller, Y., Stuart, G. & Sakmann, B. (1997). Calcium action potentials restricted to the distal apical dendrites of rat neocortical pyramidal neurons. *Journal of Physiology* **505**, 605–616.

Schwindt, P. C. & Crill, W. E. (1995). Amplification of synaptic current by persistent sodium conductance in apical dendrite of neocortical neurons. *Journal of Neurophysiology* **74**, 2220–2224.

Spain, W. J., Schwindt, P. C. & Crill, W. E. (1987). Anomalous rectification in neurons from cat sensorimotor cortex *in vitro*. *Journal of Neurophysiology* **57**, 1555–1576.

Spencer, W. A. & Kendel, E. R. (1961). Electrophysiology of hippocampal neurons. IV. Fast potentials. *Journal of Neurophysiology* **26**, 272–285.

Squire, L. R. & Zola-Morgan, S. (1991). The medial temporal lobe memory system. *Science* **253**, 1380–1386.

Staley, K. J., Otis, T. S. & Mody, I. (1992). Membrane properties of dentate gurus granule cells: comparison of sharp microelectrode and whole-cell recordings. *Journal of Neurophysiology* **67**, 1346–1358.

Stuart, G. & Sakmann, B. (1994). Active propagation of somatic action potentials into neocortical pyramidal cell dendrites. *Nature* **367**, 69–72.

Stuart, G. & Spruston, N. (1998). Determinants of voltage attenuation in neocortical pyramidal neuron dendrites. *Journal of Neuroscience* **18**, 3501–3510.

Vaughan, D. W. & Peters, A. (1973). A three dimensional study of layer I of the rat parietal cortex. *Journal of Comparative Neurology* **149**, 355–370.

Williams, S. R. & Stuart, G. J. (1999). Mechanisms and consequences of action potential burst firing in rat neocortical pyramidal neurons. *Journal of Physiology* **521**, 467–482.

Wong, R. K., Prince, D. A. & Basbaum, A. I. (1979). Intradendritic recordings from hippocampal neurons. *Proceedings of the National Academy of Sciences of the USA* **76**, 986–990.

Zeki, S. & Shipp, S. (1988). The functional logic of cortical connections. *Nature* **335**, 311–317.

Zhu, J. J. & Connors, B. W. (1999). Intrinsic firing patterns and whisker-evoked synaptic responses of neurons in the rat barrel cortex. *Journal of Neurophysiology* **81**, 1171–1183.

Zhu, J. J. & Lo, F.-S. (1999). Three GABA receptor-mediated postsynaptic potentials in interneurons in the rat lateral geniculate nucleus. *Journal of Neuroscience* **19**, 5721–5730.

Zhu, J. J. & Sakmann, B. (1997). Postnatal development of Ca^{2+}-mediated action potentials in dendritic tufts of rat neocortical pyramidal neurons. *Society for Neuroscience Abstracts* **23**, 2283.

Zhu, J. J., Uhlrich, D. J. & Lytton, W. W. (1999). Properties of a hyperpolarization-activated cation current in interneurons in the rat lateral geniculate nucleus. *Neuroscience* **92**, 445–457.

Acknowledgements

The author thanks Professor Bert Sakmann for his guidance throughout the study and manuscript preparation, Drs Hsiang-Tung Chang, Holly Cline, Gerard Borst, Alon Korngreen, Matthew Larkum, Troy Margrie, Alex Reyes and Arnd Roth for helpful comments, Dr K. Kaiser for help with initial experiments, Ms M. Kasier and Dr Y. Qin for expert technical assistance and Ms G. Dücker and Ms H. Spiegel for secretarial assistance. This study was supported by postdoctoral fellowships from the Max Planck Society.

Correspondence

J. J. Zhu: Cold Spring Harbor Laboratory, Jones 1 Bungtown Road, Cold Spring Harbor, NY 11724, USA.

Email: zhuju@cshl.org